Physics Letters B 797 (2019) 134820

Contents lists available at ScienceDirect

Physics Letters B

www.elsevier.com/locate/physletb

First experimental constraint of the spectroscopic amplitudes for the α-cluster in the ^{11}B ground state

Y.P. Shen (谌阳平)[a], B. Guo (郭冰)[a,*], T.L. Ma (马田丽)[a], D.Y. Pang (庞丹阳)[b,c], D.D. Ni (倪冬冬)[d], Z.Z. Ren (任中洲)[e], Y.J. Li (李云居)[a], Z.D. An (安振东)[f], J. Su (苏俊)[a], J.C. Liu (刘建成)[a], Q.W. Fan (樊启文)[a], Z.Y. Han (韩治宇)[a], X.Y. Li (李鑫悦)[a], Z.H. Li (李志宏)[a], G. Lian (连钢)[a], Y. Su (苏毅)[a], Y.B. Wang (王友宝)[a], S.Q. Yan (颜胜权)[a], S. Zeng (曾晟)[a], W.P. Liu (柳卫平)[a]

[a] China Institute of Atomic Energy, P. O. Box 275(10), Beijing 102413, China
[b] School of Physics and Nuclear Energy Engineering, Beihang University, Beijing 100191, China
[c] Beijing Key Laboratory of Advanced Nuclear Materials and Physics, Beihang University, Beijing 100191, China
[d] Space Science Institute, Macao University of Science and Technology, Macao, China
[e] School of Physics Science and Engineering, Tongji University, Shanghai 200092, China
[f] School of Physics and Astronomy, Sun Yat-Sen University, Zhuhai 519082, China

ARTICLE INFO

Article history:
Received 30 November 2018
Received in revised form 3 July 2019
Accepted 27 July 2019
Available online 31 July 2019
Editor: D.F. Geesaman

ABSTRACT

We present the first experimental determination on the spectroscopic amplitudes (SAs) for the α-cluster in the ^{11}B ground state via the ^{7}Li(^{6}Li, d)^{11}B reaction using a high-precision magnetic spectrograph. This is believed to have a strong effect on the studies of α-induced reactions which are crucial in nuclear astrophysics. It is found that the previous SAs of ^{11}B from shell model calculations cause overestimations of up to 23% for the ^{12}C$(\alpha,\gamma)^{16}$O $S_{E2}(300)$ factor and up to 34% for the ^{13}C$(\alpha,n)^{16}$O $S(190)$ factor with respect to the results from the present experimentally determined SAs. Due to the importance of these two reactions, for example the uncertainty in the ^{12}C$(\alpha,\gamma)^{16}$O cross section at $E_{\mathrm{c.m.}} = 300$ keV is required to be better than 10% by stellar modeling, the new S-factors could result in a potential influence on the astrophysical network calculations.

1. Introduction

A nuclear cluster can be defined as a spatially located subsystem which consists of the strongly correlated nucleons. The clustering in nuclei is one of the most fundamental aspects in nuclear structure and has been investigated since the early days in the history of nuclear physics [1]. The research of the cluster structure in light nuclei is also an interesting topic [2]. It could generate a crucial impact on the synthesis of elements in stars via cluster states like the triple-α cluster state (so-called Hoyle state) at 7.65 MeV in ^{12}C [3,4]. A cluster is characterized by its intrinsic binding stronger than the external binding. Therefore, it is possible to consider the cluster as a single unit, and to describe its behavior without reference to its internal structure. The most likely cluster is, due to its spin and isospin symmetry and hence its high binding energy, the α-particle which can propagate within a nucleus relatively unperturbed for a significant time [5]. Such a cluster can be knocked out of the nucleus by an energetic projectile, or it can be also picked up in a cluster-transfer reaction. These cluster reactions provide important information on the single-particle and on the multi-particle character of nuclear states, and thus have been widely used as powerful nuclear spectroscopic tools [6].

The α-transfer reactions, being most likely to take place by cluster transfer, not only can be utilized to investigate nuclear structure (e.g., α-decay widths [7]) and nuclear reaction mechanisms [6], but also are of particular interest for the study of astrophysical α-particle induced reactions [8] which are one kind of the most important reactions in nuclear astrophysics, since helium is the second most abundant element in the observable universe after hydrogen. Because the measurements of the α-particle induced reactions at the low-energy range are greatly hindered by the Coulomb barrier, indirect techniques (e.g., α-transfer reactions) are extremely valuable. In particular, these techniques can be used to deduce the level parameters (i.e., energies, spectroscopic factors

* Corresponding author.
E-mail address: guobing@ciae.ac.cn (B. Guo).

https://doi.org/10.1016/j.physletb.2019.134820

(SFs) or asymptotic normalization coefficients (ANC), lifetimes) that can then be used in R-matrix or other reaction model's analysis [9].

To date the α-transfer reactions induced by light nuclei, e.g. (^{6}Li, d) [10–12], (^{7}Li, t) [13,14] and (^{11}B, ^{7}Li) [15,16], have been extensively utilized to determine the above level parameters which were used to obtain stellar rates of the α-particle induced reactions including the (α,γ), (α,n) and (α,p) in stars. To obtain the above level parameters by interpreting these α-cluster transfer reactions, the spectroscopic amplitudes (SAs) or the SFs or the ANCs for the α-cluster in the ground states of these light nuclei (^{6}Li, ^{7}Li and ^{11}B) must be fixed. So far the spectroscopic information has been reasonably well determined experimentally for the ground states in ^{6}Li [17,18] and ^{7}Li [19,20], respectively. As for the SAs for the α-cluster in the ^{11}B ground state, there are two components denoted by quantum numbers $NL_j = 3S_0$ and $2D_2$, respectively, where N is the number of radial nodes that include the origin but not the infinity and L and j are the orbital and total angular momenta, respectively. The SAs of these two components are found to be -0.509 and 0.629, respectively, from a shell model calculation [21], and -0.638 and -0.422, respectively, from the translationally invariant shell model [22]. However, at present these SAs still remain unknown experimentally. Therefore, experimental determination of these SAs for the ^{11}B ground state is highly desirable.

In this letter, we report the first experimental measurement of the SAs and the ANCs of the α-cluster in the ^{11}B ground state by using a high-precision Q3D magnetic spectrograph, and evaluation of the impact of new values in comparison with two shell model calculations, by taking the two most important reactions, the $^{12}\mathrm{C}(\alpha,\gamma)^{16}\mathrm{O}$ and $^{13}\mathrm{C}(\alpha,\mathrm{n})^{16}\mathrm{O}$ reactions, for example.

2. Experiment

The experiment was performed at the HI-13 national tandem accelerator laboratory of the China Institute of Atomic Energy (CIAE) in Beijing. The experimental setup and procedures were similar to those previously reported [15,23–25]. The natural LiF with a ^{7}Li thickness of 20.2 ± 1.0 μg/cm^2 was evaporated and deposited on a self-supporting ^{12}C foil as the target. The target thickness was determined by using an analytical balance with a precision of 1 μg and was verified with the well-known differential cross sections of the d + ^{7}Li elastic scattering [26,27]. Based on the precision of the analytical balance and the error of the cross sections of the d + ^{7}Li elastic scattering, an uncertainty of 5.0% was assigned for the target thickness.

The ^{6}Li beam with an energy of 24 MeV was delivered and utilized to measure the angular distribution of the $^7\mathrm{Li}(^6\mathrm{Li},\mathrm{d})^{11}\mathrm{B}$ reaction leading to the ground state of ^{11}B and the ^{6}Li + ^{7}Li elastic scattering. The reaction products were focused and separated by the Q3D magnetic spectrograph. Six pieces of the two-dimensional position sensitive silicon detectors were installed at the focal plane of the Q3D. The two-dimensional position information from the silicon detectors enabled the products emitted into the acceptable solid angle to be completely recorded, and the energy information was used to remove the impurities with the same magnetic rigidity. As an example, Fig. 1 displays the focal-plane position spectrum of deuterium at $\theta_{\mathrm{lab}} = 5°$ from the $^7\mathrm{Li}(^6\mathrm{Li},\mathrm{d})^{11}\mathrm{B}_{\mathrm{g.s.}}$ reaction. It is seen that the spectrum is quite clear and the deuterium events from the $^7\mathrm{Li}(^6\mathrm{Li},\mathrm{d})^{11}\mathrm{B}_{\mathrm{g.s.}}$ reaction gather together well.

We performed the measurements of the cross section of the $^6\mathrm{Li} + ^7\mathrm{Li}$ elastic scattering at the energy of 24 MeV to extract the optical potential for the entrance channel of the $^7\mathrm{Li}(^6\mathrm{Li},\mathrm{d})^{11}\mathrm{B}_{\mathrm{g.s.}}$ reaction. The data of differential cross sections and the fitting curve are shown in Fig. 2. In Fig. 3, we also display the angular distribution of the $^7\mathrm{Li}(^6\mathrm{Li},\mathrm{d})^{11}\mathrm{B}_{\mathrm{g.s.}}$ reaction.

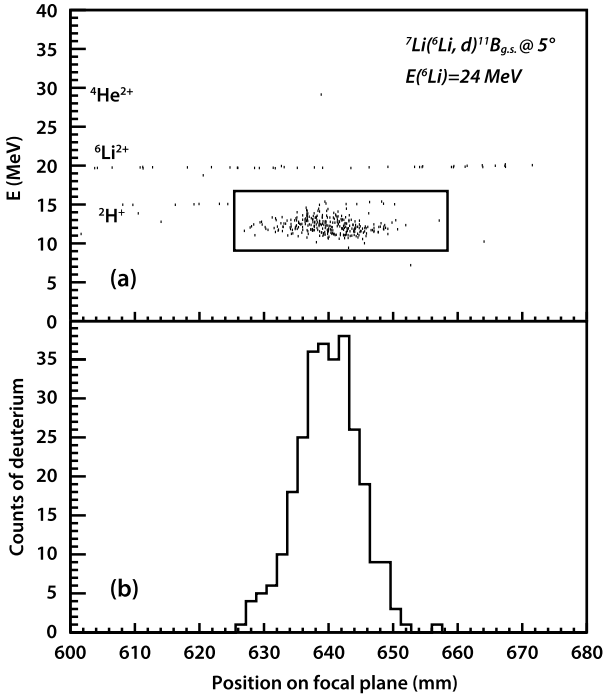

Fig. 1. Focal-plane position spectrum of deuterium at $\theta_{\mathrm{lab}} = 5°$ from the $^7\mathrm{Li}(^6\mathrm{Li},\mathrm{d})^{11}\mathrm{B}_{\mathrm{g.s.}}$ reaction. (a) Two-dimensional spectrum of energy vs. focal-plane position. (b) Spectrum gated by the deuterium events in the black window of (a).

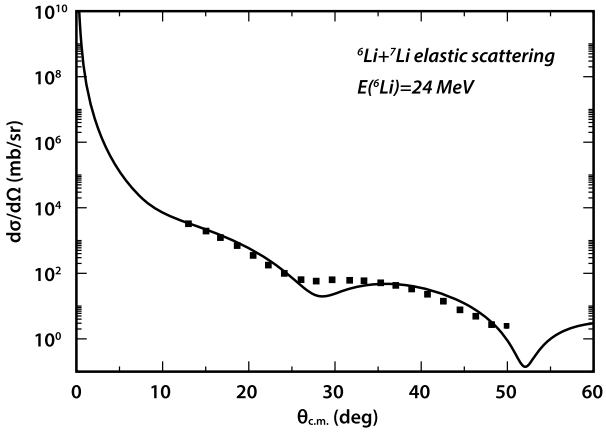

Fig. 2. The experimental data and fitting with the single-folding potential of the elastic scattering of $^6\mathrm{Li} + ^7\mathrm{Li}$.

3. Extraction of the spectroscopic amplitudes

The SAs of the $3S_0$ and $2D_2$ components in the ground state of ^{11}B were extracted with finite-range distorted wave Born approximation (DWBA) calculations. The calculations were made with the computer code FRESCO [28]. The differential cross section of the $^7\mathrm{Li}(^6\mathrm{Li},\mathrm{d})^{11}\mathrm{B}$ reaction is [29]:

$$\frac{\mathrm{d}\sigma}{\mathrm{d}\Omega} = \frac{\mu_i\mu_f}{(2\pi\hbar^2)^2}\frac{k_f}{k_i}\frac{1}{(2I_i+1)(2s_i+1)}\sum_{M_iM_f\sigma_i\sigma_f}|T|^2, \qquad (1)$$

where μ_i and μ_f and k_i and k_f are the reduced masses and the asymptotic momenta in the entrance and the exit channels, respectively, I_i and s_i are the spins of the target and the projectile, and M_i, M_f, σ_i, and σ_f are the z-components of the target and the projectile in the entrance and exit channels. The transition amplitude T reads:

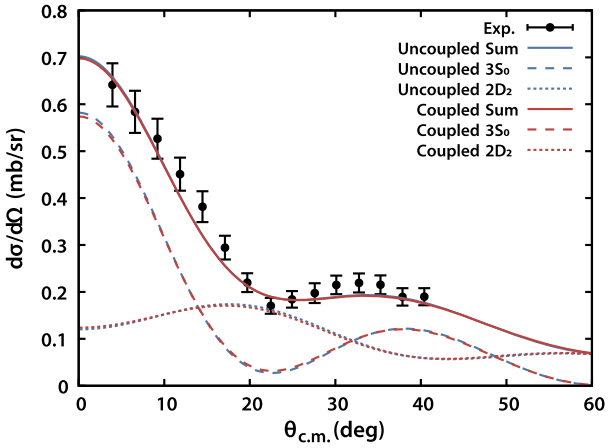

Fig. 3. Angular distribution of the ^{7}Li(^{6}Li, d)^{11}B$_{g.s.}$ reaction. The red and blue lines represent the normalized DWBA calculations with coupled and uncoupled α + ^{7}Li wave functions. The solid lines are the incoherent sums of the $3S_0$ and $2D_2$ components. The dashed line and the dotted line are the cross sections from the contribution of the $3S_0$ and $2D_2$ components in the ^{11}B ground state, respectively.

$$T = \langle \chi_f^{(-)}(\alpha\phi_{3S_0} + \beta\phi_{2D_2}) \left| V_{d^7Li} + V_{d\alpha} - V_{d^{11}B} \right| \gamma\phi_{d\alpha}\chi_i^{(+)} \rangle$$
$$= T_S + T_D, \quad (2)$$

$$T_S = \alpha\gamma \langle \chi_f^{(-)}\phi_{3S_0} \left| V_{d^7Li} + V_{d\alpha} - V_{d^{11}B} \right| \phi_{d\alpha}\chi_i^{(+)} \rangle, \quad (3)$$

$$T_D = \beta\gamma \langle \chi_f^{(-)}\phi_{2D_2} \left| V_{d^7Li} + V_{d\alpha} - V_{d^{11}B} \right| \phi_{d\alpha}\chi_i^{(+)} \rangle, \quad (4)$$

where χ_i and χ_f are the distorted waves in the entrance and exit channels, ϕ_{3S_0}, ϕ_{2D_2}, and $\phi_{d\alpha}$ are the wave functions of the $3S_0$ and $2D_2$ components in the ^{11}B ground state and the ^{6}Li = d + α system, α, β, and γ are the SAs of the $3S_0$ and $2D_2$ components in the ground state of ^{11}B and the SA of the α-particle in the ground state of ^{6}Li, and α^2, β^2, and γ^2 are the corresponding SFs. V_{ij} are the two-body interactions between particles i and j. Since the contributions of the $3S_0$ and $2D_2$ components add incoherently in DWBA calculations, the differential cross section of the ^{7}Li(^{6}Li, d)^{11}B reaction can be further written as:

$$\frac{d\sigma}{d\Omega} = \gamma^2 \left[\alpha^2 \left(\frac{d\sigma}{d\Omega} \right)_{3S_0} + \beta^2 \left(\frac{d\sigma}{d\Omega} \right)_{2D_2} \right], \quad (5)$$

where $(d\sigma/d\Omega)_{3S_0}$ and $(d\sigma/d\Omega)_{2D_2}$ are the differential cross sections of the $3S_0$ and $2D_2$ components, respectively.

Model parameters required in these calculations include the optical model potentials (OMPs) of the entrance- and exit-channels, the core-core (d + ^{7}Li) interaction, and the real binding potentials for the (^{6}Li = α + d) and the (^{11}B = α + ^{7}Li) systems. The entrance channel OMP was obtained by folding the nucleon density distributions of ^{6}Li and ^{7}Li with the systematic nucleon-nucleus potential of the JLMB model [30] as those done in Refs. [31,32]. The density distributions of ^{6}Li and ^{7}Li were obtained with the independent-particle model [33]. A systematic analysis of the differential cross sections of ^{6}Li and ^{7}Li elastic scattering from ^{6}Li, ^{7}Li, ^{9}Be, and ^{10}B targets at incident energies ranging from 7 MeV to 44 MeV was made. All the data sets are listed in Table 1. Optimal renormalization factors, N_r and N_i, for the real and imaginary parts of the folding potentials, respectively, were determined by globally fitting all datasets with the standard minimum χ^2 method. The results are $N_r = 0.694 \pm 0.023$ and $N_i = 0.967 \pm 0.025$. These N_r and N_i values account reasonably well for the elastic scattering of ^{6}Li from ^{7}Li at 24 MeV. A comparison between the results of optical model calculations and the experimental data is shown in Fig. 2. For the exit-channel OMP corresponding to the d + ^{11}B system, we adopted the recent systematic deuteron potential by Zhang et al. [34], which was specifically obtained for deuteron scattering from the 1p-shell nuclei. The transfer cross sections were calculated with a full complex remnant term in the transition amplitude. The core-core potential (for the d + ^{7}Li system) was also taken from Zhang et al. [34].

Table 1
The 36 sets of experimental elastic scattering data and their references included in the determination of the optical potential for ^{6}Li + ^{7}Li system.

System	References	E_{lab} (MeV)
^{6}Li + ^{6}Li	Potthast (1997) [35]	10, 15, 20, 25, 30, 35, 40
^{6}Li + ^{7}Li	Potthast (1998) [36]	10, 15, 20, 25, 30, 35, 40
	Momotyuk (2006) [37]	42
	Su (2010) [38]	44
	Present	24
^{6}Li + ^{9}Be	Muskat (1995) [39]	7, 10, 12
^{7}Li + ^{7}Li	Bachmann (1993) [40]	8-17
	Momotyuk (2006) [37]	42
	Parkar (2009) [41]	20, 25
^{7}Li + ^{9}Be	Verma (2010) [42]	24, 30
^{7}Li + ^{10}B	Etchegoyen (1988) [43]	39

The real α-d potential in the ground state of ^{6}Li is of typical Woods-Saxon form. The radius and diffuseness parameters, R_0 and a, were adjusted so that the corresponding root-mean-square (rms) radius of the α-cluster wave function, $\sqrt{\langle r^2 \rangle}$, satisfied the following relation which was also applied in Guo et al. (2012) [15],

$$\left\langle r_{com}^2 \right\rangle = \frac{m_\alpha}{m_{com}} \left\langle r_\alpha^2 \right\rangle + \frac{m_c}{m_{Li}} \left\langle r_c^2 \right\rangle + \frac{m_c m_\alpha}{m_{com}^2} \left\langle r^2 \right\rangle, \quad (6)$$

where $\langle r_c^2 \rangle$, $\langle r_\alpha^2 \rangle$, and $\langle r_{com}^2 \rangle$ are the mean-square radii of the core, the α particle, and the composite nucleus, respectively. The depth of this potential was determined with the usual separation energy prescription. For the ground state of ^{6}Li, in which the wave function of the α cluster has only one component, $\sqrt{\langle r_c^2 \rangle}$, $\sqrt{\langle r_\alpha^2 \rangle}$, and $\sqrt{\langle r_{com}^2 \rangle}$ were taken to be 1.95 fm, 1.47 fm and 2.46 fm, respectively [44]. They correspond to $\sqrt{\langle r^2 \rangle} = 3.879$ fm, which is satisfied when $R_0 = 2.7$ fm and $a = 0.4$ fm. The ground state of ^{11}B is relatively more complicated. The radial wave functions of its $3S_0$ and $2D_2$ components were obtained through the coupled-channel calculations, which was developed by Ni and Ren (2011) [45] (also see Delion et al. (2018) [46] for a review), with a deformed Woods-Saxon potential assuming a quadrupole deformation of the core nucleus ^{7}Li:

$$V(r, \theta) = \frac{V_0}{1 + \exp[(r - R(\theta))/a]}. \quad (7)$$

Here $R(\theta) = R_0 + \delta_2(^{7}\text{Li})Y_{20}(\theta)$ and $\delta_2(^{7}\text{Li})$ is the quadrupole deformation length of ^{7}Li which was taken to be 2.0 fm from Cook et al. (1987) [47]. The rms radii of the coupled $3S_0$ and $2D_2$ wave functions satisfy Eq. (6) with the rms radii of the core and the composite nuclei, ^{7}Li and ^{11}B, being 2.384 fm [44] and 2.605 fm [48], respectively. The resulting values of R_0 and a are 3.15 fm and 0.6 fm, respectively. In order to see the coupling effects, comparisons are made with calculations with the $3S_0$ and $2D_2$ wave functions obtained from uncoupled equations. We require the rms radii of the uncoupled $3S_0$ and $2D_2$ wave functions to satisfy the same relation in Eq. (6) as well, which is supported by the parameters $R_0 = 3.43$ fm and $a = 0.60$ fm.

Results of the DWBA calculations with both coupled and uncoupled $3S_0$ and $2D_2$ wave functions for the ^{7}Li(^{6}Li, d)^{11}B reaction are shown in Fig. 3. Both cross sections from the individual contributions of the $3S_0$ and $2D_2$ components and their incoherent sums are presented. The differences in the angular distributions with the

Table 2
List of the uncertainties in the SAs for the ^{11}B ground states.

Uncertainty source	Relative error	
	$2D_2$	$3S_0$
Entrance channel potential	2.1%	1.5%
Exit channel potential	5.1%	8.3%
(α + d) binding potential	8.9%	3.5%
(α + ^{7}Li) binding potential	5.2%	3.4%
ANC for $\alpha + \mathrm{d} \rightarrow {}^6$Li	4.7%	4.7%
Target thickness	5.0%	5.0%
Statistics	2.6%	2.8%
Total	13.8%	12.2%

coupled and uncoupled $3S_0$ and $2D_2$ wave functions should be attributed to the slight differences in the radial shapes of their wave functions. It's seen that calculations with both coupled and uncoupled $3S_0$ and $2D_2$ wave functions account for the experimental data reasonably well. The good agreement between our calculated and measured angular distributions gives strong evidence of the direct nature of the ^{7}Li(^{6}Li, d)^{11}B$_{\mathrm{g.s.}}$ reaction at this energy.

To obtain the SAs and the ANCs of the α-cluster for the ground state of ^{11}B, the SA or the ANC of the α-cluster in the ground state of ^{6}Li needs to be fixed. We adopt the ANC for ^{6}Li reported in Refs. [17,18], which has $(C^{^6\mathrm{Li}}_{\alpha\mathrm{d}})^2 = 5.3 \pm 0.5$ fm^{-1}. The SF for ^{6}Li was then deduced with the relation $C^2 = S_\alpha b^2$ where b is the single-particle ANC [49]. Under these conditions, we are able to determine the SAs and ANCs for the $3S_0$ and $2D_2$ components in the ground state of ^{11}B by normalizing the DWBA cross section to the experimental one. Even being solutions of the coupled equations, the coupled $3S_0$ and $2D_2$ wave function may still be too simple to represent the real nature of ^{11}B. With such a consideration, we extracted the SAs of the $3S_0$ and $2D_2$ components for both the coupled and uncoupled cases by requiring the incoherent sum of the $3S_0$ and $2D_2$ cross sections to best reproduce the experimental ones. The uncertainties in these SAs are listed in Table 2. The resulting SAs for the $3S_0$ and $2D_2$ components are 0.64 ± 0.09 and 0.74 ± 0.09, respectively for the uncoupled case. Their corresponding ANC values are $(1.29 \pm 0.18) \times 10^4$ fm^{-1} and $(4.02 \pm 0.49) \times 10^3$ fm^{-1}, respectively. For the coupled case, the SAs are 0.66 ± 0.09 and 0.73 ± 0.09, and the ANCs are $(1.38 \pm 0.19) \times 10^4$ fm^{-1} and $(3.97 \pm 0.48) \times 10^3$ fm^{-1}, respectively. It is seen that the differences in the SAs obtained with the coupled and uncoupled calculations of the $3S_0$ and $2D_2$ wave functions differ by less than 4%. This indicates that the coupled wave function can be rather well approximated by the uncoupled ones in DWBA calculations when both wave functions subject to the same constraints from the rms radii of the composite nucleus and its constituent clusters according to Eq. (6). This would be very useful for analysis of the other α-cluster transfer reactions.

4. Impact on the astrophysical ^{12}C(α, γ)^{16}O and ^{13}C(α, n)^{16}O reactions

It is seen that our results of the SAs for the ^{11}B ground state, which are $(0.64 \pm 0.09,\ 0.74 \pm 0.09)$ and $(0.66 \pm 0.09,\ 0.73 \pm 0.09)$, largely differ from the shell model calculations by Kurath et al. (1973) [21] $(-0.509,\ 0.629)$ and Rudchik et al. (2005) [22] $(-0.638,\ -0.422)$. This would lead to significant influence on the SFs or ANCs for the states of astrophysical relevance obtained from the (^{11}B, ^{7}Li) transfer reaction, and then on the cross sections of the astrophysical reactions. Thus, we reanalyzed the angular distributions of the ^{12}C(^{11}B, ^{7}Li)^{16}O reaction from [50] and the ^{13}C(^{11}B, ^{7}Li)^{17}O reaction from [15] and evaluated the impacts of our new SFs on the ^{12}C(α, γ)^{16}O and ^{13}C(α, n)^{16}O reactions which are the two of the most important reactions in nuclear astrophysics. The DWBA angular distributions for each reaction were calculated to show the differences among their absolute values and were normalized to the experimental data to compare their shapes. The results are shown in Fig. 4. The SFs and the ANCs (C^2 and $\tilde{C}^2$) for the ^{16}O 6.917 MeV 2^+ state and the ^{17}O 6.356 MeV $1/2^+$ state were also obtained using the ^{11}B SAs from Kurath et al. (1973) [21], Rudchik et al. (2005) [22] and the present work by the normalization of the DWBA calculations to the ^{12}C(^{11}B, ^{7}Li)^{16}O and ^{13}C(^{11}B, ^{7}Li)^{17}O data from Shen et al. [50] and Guo et al. [15]. The present SFs or ANCs are in agreement with those from the (^{6}Li, d) and (^{7}Li, t) reactions [13,14,51–54].

When comparing the SAs for the ^{11}B ground state from Kurath et al. (1973) [21] and the present work, we can see that a similar ratio of the $3S_0$ to $2D_2$ components was given. This means the DWBA angular distributions from these two results will show a similar shape, as shown in Fig. 4 (b) and (d). However, the absolute values of the angular distributions with the Kurath's SAs are smaller than those with the present one, as shown in Fig. 4 (a) and (c). The Rudchik's work [22] gives a similar SA for $3S_0$ component in ^{11}B ground state, but gives a much smaller value of the $2D_2$ component than the present result. Therefore, the shape of the DWBA angular distribution obtained with the Rudchik's SAs is different and the absolute value of the angular distribution is smaller than the present one. Thus, the newly deduced SFs and ANCs of the ^{16}O 6.917 MeV 2^+ state and the ^{17}O 6.356 MeV $1/2^+$ state were smaller than those obtained with Kurath's and the Rudchik's SAs. The new SFs and ANCs exhibit significant decreases by a factor of up to 1.60 for the ^{16}O 6.917 MeV 2^+ state, and a factor of up to 1.58 for the ^{17}O 6.356 MeV $1/2^+$ state. The results are listed in Table 3.

In order to show the impact of the new SFs or ANCs, we derived the astrophysical $S_{E2}(300)$ factor of the ^{12}C(α, γ)^{16}O reaction by considering the ^{16}O 6.917 MeV 2^+ subthreshold resonance and six resonances with the R-matrix method, and extracted the $S(190)$ factor of the ^{13}C(α, n)^{16}O reaction by considering the ^{17}O 6.356 MeV $1/2^+$ subthreshold resonance and eleven resonances with the Breit-Wigner formula, by following the same procedures as those by Shen et al. [50] and Guo et al. [15]. The comparison is also listed in Table 3. Comparing with the present results, the $S_{E2}(300)$ factor for the ^{12}C(α, γ)^{16}O reaction deduced with shell model results shows an overestimate of up to 23% and the $S(190)$ factor for the ^{13}C(α, n)^{16}O reaction shows an overestimate of up to 34%. Due to the importance of these two reactions, for example an uncertainty of better than 10% in the ^{12}C(α, γ)^{16}O cross section at $E_{\mathrm{c.m.}} =$ 300 keV is required by stellar modeling [9,55], the new S-factors could have a potential influence on the astrophysical network calculations.

5. Summary and conclusion

The α-transfer reactions are of particular interest for the study of the astrophysical α-particle induced reactions which are one kind of the most important reactions in nuclear astrophysics. In addition to (^{6}Li, d) and (^{7}Li, t), the (^{11}B, ^{7}Li) reaction has been extensively utilized to investigate the α-particle induced reactions occurred in stars. However, the SAs for the α-cluster in the ground state of ^{11}B, which are required when interpreting α-cluster transfer reactions, still remain unknown experimentally. This largely puts application of the (^{11}B, ^{7}Li) reactions in doubt.

In this work, we present the angular distribution of the ^{7}Li(^{6}Li, d)^{11}B$_{\mathrm{g.s.}}$ reaction measured using a high-precision magnetic spectrograph. The SAs of the $3S_0$- and $2D_2$-wave components of the α cluster in the ground state of ^{11}B were extracted by requiring the summation of the $3S_0$- and $2D_2$-wave cross sections to best reproduce the experimental data in a DWBA analysis. The $3S_0$

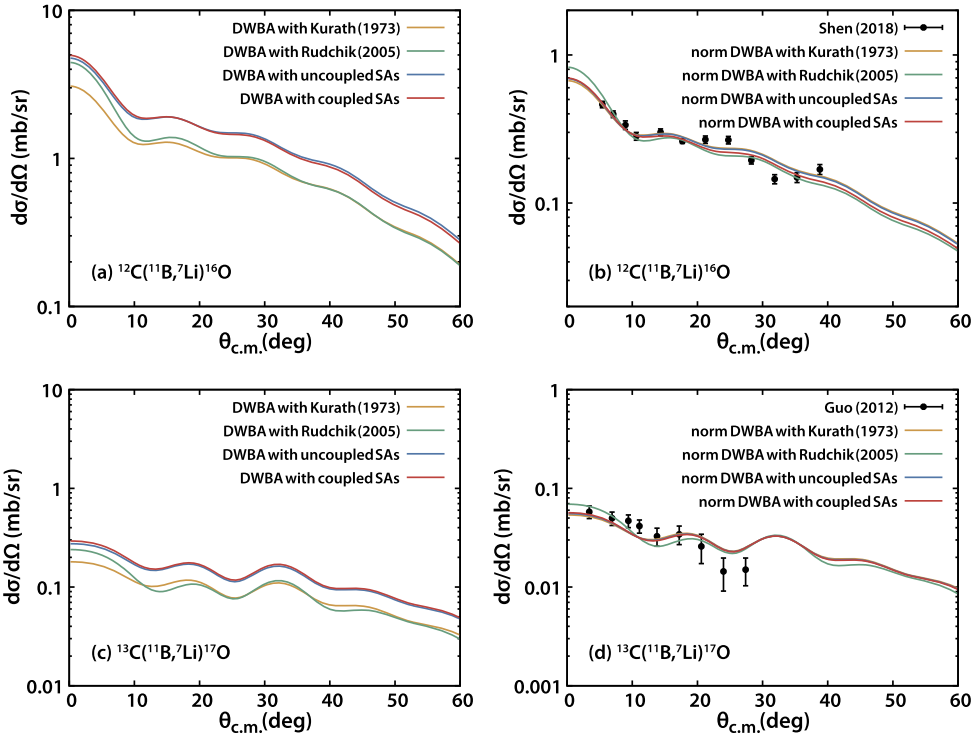

Fig. 4. Impact on the DWBA calculation of the ^{12}C(^{11}B, ^{7}Li)^{16}O and ^{13}C(^{11}B, ^{7}Li)^{17}O reactions. (a) and (c) present the DWBA angular distributions, without any normalization, of the ^{12}C(^{11}B, ^{7}Li)^{16}O and ^{13}C(^{11}B, ^{7}Li)^{17}O reactions, respectively. (b) and (d) show the normalized DWBA results to the experimental data of the ^{12}C(^{11}B, ^{7}Li)^{16}O reaction populating the 6.917 MeV subthreshold state in ^{16}O from Shen et al. (2018) [50] and the ^{13}C(^{11}B, ^{7}Li)^{17}O reaction populating the 6.356 MeV subthreshold state in ^{17}O from Guo et al. (2012) [15], respectively. The coupled and uncoupled SAs denote the present SAs for the ^{11}B ground states with coupled and uncoupled $\alpha + {}^{7}$Li wave functions.

Table 3
List of the SFs and the ANCs (C^2 and $\tilde{C}^2$) for the ^{16}O 6.917 MeV 2^+ state and the ^{17}O 6.356 MeV $1/2^+$ state obtained using the ^{11}B SAs from Kurath et al. (1973) [21], Rudchik et al. (2005) [22] and the present work by fitting the ^{12}C(^{11}B, ^{7}Li)^{16}O and ^{13}C(^{11}B, ^{7}Li)^{17}O angular distributions from Shen et al. [50] and Guo et al. [15], respectively. "Uncoupled" and "Coupled" denote the present results with the uncoupled and coupled ^{11}B SAs, respectively. The $\tilde{C}^2$ represents the square of the Coulomb modified ANC which is define as $\tilde{C}^2 = C^2/\Gamma(L+1+\eta)^2$. Also the astrophysical $S_{E2}(300)$ factors for the ^{12}C(α,γ)^{16}O reaction and the $S(190)$ factor for the ^{13}C(α, n)^{16}O reaction are listed in the table. The columns of the "RTP" show the ratios of the S-factors with respect to the present coupled results.

	^{16}O 6.917 MeV 2^+				^{17}O 6.356 MeV $1/2^+$			
	SF	C^2 (10^{10} fm^{-1})	$S_{E2}(300)$ (keV b)	RTP	SF	$\tilde{C}^2$ (fm^{-1})	$S(190)$ (10^6 MeV b)	RTP
Kurath (1973) [21]	0.214 ± 0.054	1.62 ± 0.41	56.0 ± 9.3	1.23	0.38 ± 0.12	4.1 ± 1.1	1.38 ± 0.25	1.34
Rudchik (2005) [22]	0.181 ± 0.044	1.37 ± 0.34	52.7 ± 8.8	1.16	0.37 ± 0.12	3.9 ± 1.1	1.34 ± 0.24	1.30
Uncoupled	0.146 ± 0.038	1.10 ± 0.29	46.2 ± 7.7	1.02	0.252 ± 0.076	2.74 ± 0.77	1.07 ± 0.18	1.04
Coupled	0.133 ± 0.034	1.01 ± 0.25	45.4 ± 7.6	1	0.240 ± 0.076	2.58 ± 0.70	1.03 ± 0.16	1

and $2D_2$ wave functions are obtained as solutions of both coupled and uncoupled equations. It is found that the difference between the experimental SAs extracted with the coupled and uncoupled wave functions is less than 4% when the same rms radii constraint is satisfied. This indicates that the uncoupled wave functions are good approximations to the coupled ones and can be used in the study of the other α-cluster transfer reactions.

We also studied the impact of the new ^{11}B SAs on two astrophysical key reactions, ^{12}C(α,γ)^{16}O and ^{13}C(α, n)^{16}O. Our experimental SAs for the ^{11}B ground state yield significant decreases of the SFs or the ANCs in the 6.917 MeV 2^+ subthreshold state in ^{16}O (by a factor of up to 1.60) and in the 6.356 MeV $1/2^+$ subthreshold state in ^{17}O (by a factor of up to 1.58) when comparing with the ones obtained with the shell model SAs. Consequently, our results indicate significant overestimates of up to 23% for the astrophysical $S_{E2}(300)$ factor of the ^{12}C(α,γ)^{16}O reaction, and of up to 34% for the $S(190)$ factor of the ^{13}C(α, n)^{16}O reaction by the shell model results. Due to the importance of these two reactions and the precision requirements of the stellar modeling, the new S-factors could result in a potential influence on the astrophysical network calculations.

Acknowledgements

The authors thank the staff of the HI-13 tandem accelerator for the smooth operation of the machine. This work was supported by the National Key Research and Development Project under Grant No. 2016YFA0400502, the National Natural Science Foundation of China under Grants No. 11490561, 11475264, 11535004, 11775013 and 11761161001, the 973 program of China under Grant No. 2013CB834406 and the Science and Technology Development Fund of Macao under Grant No. 008/2017/AFJ.

References

[1] L.R. Hafstad, E. Teller, Phys. Rev. 54 (1938) 681.
[2] B. Zhou, et al., Phys. Rev. Lett. 110 (2013) 262501.
[3] F. Hoyle, Astrophys. J. Suppl. Ser. 1 (1954) 121.
[4] P. Schuck, et al., Phys. Scr. 91 (2016) 123001.
[5] M. Freer, Rep. Prog. Phys. 70 (2007) 2149.

[6] P. Hodgson, E. Beták, Phys. Rep. 374 (2003) 1.
[7] D.F. Jackson, M. Rhoades-Brown, Nature 267 (1977) 593.
[8] L. Buchmann, et al., Astrophys. J. 324 (1988) 953.
[9] R.J. deBoer, et al., Rev. Mod. Phys. 89 (2017) 035007.
[10] E.D. Johnson, et al., Phys. Rev. Lett. 97 (2006) 192701.
[11] S. Adhikari, C. Basu, Phys. Lett. B 704 (2011) 308.
[12] M.L. Avila, et al., Phys. Rev. C 90 (2014) 042801.
[13] M.G. Pellegriti, et al., Phys. Rev. C 77 (2008) 042801.
[14] N. Oulebsir, et al., Phys. Rev. C 85 (2012) 035804.
[15] B. Guo, et al., Astrophys. J. 756 (2012) 193.
[16] S.Y. Mezhevych, et al., Phys. Rev. C 95 (2017) 034607.
[17] R.G.H. Robertson, et al., Phys. Rev. Lett. 47 (1981) 1867.
[18] L.D. Blokhintsev, et al., Phys. Rev. C 48 (1993) 2390.
[19] M.E. Cobern, et al., Phys. Rev. C 14 (1976) 491.
[20] P. Mohr, et al., Phys. Rev. C 48 (1993) 1420.
[21] D. Kurath, Phys. Rev. C 7 (1973) 1390.
[22] A.A. Rudchik, et al., Phys. Rev. C 72 (2005) 034608.
[23] B. Guo, et al., Phys. Rev. C 89 (2014) 012801(R).
[24] Y.J. Li, et al., Eur. Phys. J. A 48 (2012) 1.
[25] Z.H. Li, et al., Phys. Rev. C 87 (2013) 017601.
[26] H. Lüdecke, et al., Nucl. Phys. A 109 (1968) 676.
[27] H. Bingham, et al., Nucl. Phys. A 173 (1971) 265.
[28] I.J. Thompson, Comput. Phys. Rep. 7 (1988) 167.
[29] N. Austern, Direct Nuclear Reaction Theories, John Wiley and Sons, New York, 1970.
[30] E. Bauge, et al., Phys. Rev. C 63 (2001) 024607.
[31] D.Y. Pang, et al., Phys. Rev. C 83 (2011) 064619.
[32] Y.P. Xu, D.Y. Pang, Phys. Rev. C 87 (2013) 044605.
[33] G.R. Satchler, Nucl. Phys. A 329 (1979) 233.
[34] Y. Zhang, et al., Phys. Rev. C 94 (2016) 014619.
[35] K.W. Potthast, et al., Nucl. Phys. A 614 (1997) 95.
[36] K.W. Potthast, et al., Nucl. Phys. A 629 (1998) 656.
[37] O. Momotyuk, et al., Phys. Lett. B 640 (2006) 13.
[38] J. Su, et al., Chin. Phys. Lett. 27 (2010) 052101.
[39] E. Muskat, et al., Nucl. Phys. A 581 (1995) 42.
[40] A.M. Bachmann, et al., Z. Phys. A 346 (1993) 47.
[41] V.V. Parkar, et al., Pramana J. Phys. 72 (2009) 363.
[42] S. Verma, et al., Eur. Phys. J. A 44 (2010) 385.
[43] A. Etchegoyen, et al., Phys. Rev. C 38 (1988) 2124.
[44] E. Liatard, et al., Europhys. Lett. 13 (1990) 401.
[45] D.D. Ni, Z.Z. Ren, Phys. Rev. C 83 (2011) 067302.
[46] D.S. Delion, et al., J. Phys. G 45 (2018) 053001.
[47] J. Cook, et al., Nucl. Phys. A 466 (1987) 168.
[48] Y. Funaki, et al., Prog. Part. Nucl. Phys. 82 (2015) 78.
[49] D.Y. Pang, A.M. Mukhamedzhanov, Phys. Rev. C 90 (2014) 044611.
[50] Y.P. Shen, et al., Phys. Rev. C 99 (2019) 025805.
[51] C.R. Brune, et al., Phys. Rev. Lett. 83 (1999) 4025.
[52] A. Belhout, et al., Nucl. Phys. A 793 (2007) 178.
[53] M.L. Avila, et al., Phys. Rev. Lett. 114 (2015) 071101.
[54] N. Keeley, et al., Nucl. Phys. A 726 (2003) 159.
[55] T.A. Weaver, S.E. Woosley, Phys. Rep. 227 (1993) 65.